Materials Performance and Characterization, Vol. 1, No. 1
Paper ID MPC20120017
www.astm.org

Sergio F. Gueijman,[1] *Carlos E. Schvezov,*[2] *and Alicia E. Ares*[3]

Tracking Interphases in Directionally Solidified Zn-Al Binary Alloys

REFERENCE: Gueijman, Sergio F., Schvezov, Carlos E., and Ares, Alicia E., "Tracking Interphases in Directionally Solidified Zn-Al Binary Alloys," *Materials Performance and Characterization*, Vol. 1, No. 1, 2012, pp. 1–16, doi:10.1520/MPC20120017. ISSN 2165-3992.

ABSTRACT: In the present work, we investigated the movement of [liquid/(solid + liquid)] interphases [L/(S + L)], [(solid + liquid)/(eutectic + solid + liquid)] interphases [(S + L)/(E + L)], [(eutectic + solid + liquid)/solid] interphases [(E + L)/S], and [(solid + liquid)/solid] interphases [(S + L)/S], running in a binary Zn-Al alloy system from the chilled ends of a hemicylindrical sample. We found that under specific solidification conditions, new [(S + L)/(E + L)] and [(S + L)/S] interphases can be created in the center of the sample, and then move toward the ends of the probe and collide with the solidification advancing fronts. In a horizontal setup with chilled ends we determined the speeds and accelerations of the four imposed interphases, two of which moved from left to right and two of which moved from right to left. We were also able to detect the creation of new [(S + L)/(E + L)] and [(E + L)/S] or [(S + L)/S] interphases created near the center of the sample, and to calculate their speeds and accelerations from the near beginning of the creation to the instant in which they collided with the imposed solidification fronts.

KEYWORDS: directional solidification, zinc-aluminum alloys, interphases of solidification, interphase boundary dynamics, phase transformations

Nomenclature

[L/(S + L)] = interphase which separates the fully liquid phase from the (solid + liquid) or mushy phase. It is assumed that it is at the non-equilibrium liquidus temperature when solidification occurs under non-equilibrium conditions

[(S + L)/(E + L)] = interphase which delimitates the (solid + liquid) or mushy phase from the (eutectic + solid + liquid) phase and it is assumed to be at the beginning of the eutectic plateau or Eutectic temperature under non-equilibrium conditions

[(E + L)/S] = interphase which delimitates the (eutectic + solid + liquid) phase from the completely solid phase and it is assumed that it can be found at the end of the eutectic plateau at the non-equilibrium eutectic temperature

[(S + L)/S] = interphase which delimitates the (liquid + solid) phase from the completely solid phase and it is assumed to be at the non-equilibrium solidus temperature

Manuscript received September 29, 2011; accepted for publication July 27, 2012; published online September 2012.

[1]Professor at the School of Sciences, Univ. of Misiones, 1552 Félix de Azara St., 3300 Posadas -Misiones, Argentina, e-mail: sgueijman@gmail.com

[2]Member of the Scientific Research Career (CIC) of the National Science Research Council of Argentina (CONICET); and Professor at the School of Sciences, Univ. of Misiones, 1552 Félix de Azara St., 3300 Posadas-Misiones, Argentina, e-mail: schvezov@fceqyn.unam.edu.ar

[3]Member of the Scientific Research Career (CIC) of the National Science Research Council of Argentina (CONICET); and Professor at the School of Sciences, Univ. of Misiones, 1552 Félix de Azara St., 3300 Posadas-Misiones, Argentina (Corresponding author), e-mail: aares@fceqyn.unam.edu.ar

Introduction

Most of the mathematics used to describe the physics underlying solidification models addresses the issue of determining the speed of the solid/liquid "interfaces" at the microscopic level. The determination of such speeds depends on the radius tip, imposed temperature gradients, solute segregation, supercooling, tip undercooling, and so on. Speed growth has been measured in transparent materials [1,2] and alloys [3], but most of the measurements and calculations have been carried out looking either at the dendrite tip or at the surface of the moving solid/liquid interface using expensive synchrotron X-ray techniques [3,4], radiography [5,6], and topography [7]. It is of major interest to be able to determine the solidification process in situ and in real time, since the phenomena of alloy solidification are dynamical. In the present work, we used thermocouple measurements to track the moving interphases; however, these measurements cannot be used to track dendrite tips nor solid/liquid surfaces, since temperature measurements are determined from a small volume and not a surface. In addition, we used temperature measurements to track averaged [L/(S + L)] interphases and [(S + L)/S] interphases but not solid/liquid "interfaces"; thus dendrite tip surfaces or equiaxed grain surfaces may be in whichever (solid + liquid) region. We assumed that solid cannot exist ahead the [L/(S + L)] interphase and that liquid cannot exist backward the [(S + L)/S] interphase nor the [(E + L)/S] interphase. It is only in the mushy (solid + liquid) zone where all the "interfaces" do exist, and the mushy zone is at temperatures between the liquidus and solidus (or eutectic) temperatures. Given a heat flux or imposing gradients at the ends of a liquid sample, the first two [L/(S + L)] interphases are created at each end and can move freely toward the center of the sample until they collide somewhere in the sample. The last two [(S + L)/S] or [(E + L)/S] interphases are created later when the ends of the sample reach the solidus (or eutectic) temperature and can move towards the center of the sample where they finally collide. In a previous work [8] we found that the geometric point (or surface) where [L/(S + L)] interphases collide may not be (and generally is not) the same geometric point (or surface) where [(S + L)/S] interphases do. This is also true for [(S + L)/(E + L)] interphases, which can collide in any region inside a directionally solidified sample. It is not a coincidence that the two [L/(S + L)] interphases collide at a given point (or surface) near the center of the sample. It is true if the imposed gradients are the same at both ends, they vary in the same manner during time, and there is some kind of symmetry in the sample, so one end might be considered to be a specular image of the other end.

However, [(S + L)/S] interphases move into a mushy zone that is usually highly anisotropic and inhomogeneous. Therefore, although the imposed gradients or the heat flux specified could be nearly the same at both ends, they will move at different speeds and accelerations and will collide at a different point (or surface) inside the sample. Usually, this point (or surface) is not the same geometric point (or surface) in which the previous interphases met.

Moreover, if near the middle of the sample the temperature is always above the Solidus (or Eutectic) temperature, there will be only two [(S + L)/S] interphases. However, if the sample reaches a eutectic and nearly constant temperature near the middle of the sample, new [(S + L)/S] interphases can be born near the middle of the sample at a given point (or surface) into the mushy zone. Thus, fully solidification can occur first in the middle centre of the sample, while two mushy zones remain in-between both ends. This can lead to the problem of premature freezing (namely cold shuts). These two new interphases can move toward the ends of the sample until they collide with the other two advancing interphases. Thus, four [(S + L)/S] interphases may coexist in the sample during directional solidification, although, of course, the number of solid/liquid "interfaces"

in the mushy zone may be much higher than that. Furthermore, if a eutectic plateau is reached and there is a nearly constant temperature inside the sample, [(S + L)/(E + L)] interphases can be born near the middle of the sample at a given point (or surface) in the mushy zone. Thus, four [(S + L)/(E + L)] interphases may coexist in the sample during directional solidification. As a consequence of these newly discovered interphases, we found that there are many solidification assumptions that could not be applied to adequately describe the solidification behaviour.

In the present work, we focused on the solidification of Zn-Al alloys because they are widely used in the industry. The main objective was to determine the kinetics of the interphases, as well as their speeds, accelerations, and collision points (or surfaces) when binary alloys are solidified under one-directional solidification in a horizontal setup extracting heat from both ends.

Experimental Setup

Figure 1 shows a schematic drawing of the experimental setup. Small hemicylindrical probes 140 mm long of Zn-Al alloy (i.e., Zn-1% wt. Al) were solidified in a horizontal electric furnace. The heat flux toward the ends of the sample was obtained by two cooling systems located at the ends of the ceramic crucible. The temperatures at eight different positions were measured using a TC 7003 C acquisition system and recorded every 10 s (nearly 1.25 s per channel) using a SensorWatch software in a compatible PC from the onset until the end of solidification. Alloys were prepared with high purity metals (electrolytic Zinc 99.999 wt. % and commercial grade Aluminum 99.9 wt. %). The alloy was first melted and mixed in a conventional furnace, poured into a previously heated ceramic crucible. The crucible with the alloy was put into the horizontal oven and heated above the melting point of the alloy. The solidification of the sample was obtained by cooling down the alloy using the cooling system which extracts the heat toward both ends. Just before solidification started, the cooling rate at the ends was (0.25 ± 0.05) K/s at the left end and (0.15 ± 0.05) K/s at the right end. It is important to point out that some radial heat flux can exist, but that the solidification was predominantly one-directional since the axial heat flux was greater than the radial heat flux. The hemicylindrical samples were then sectioned on a mid-longitudinal

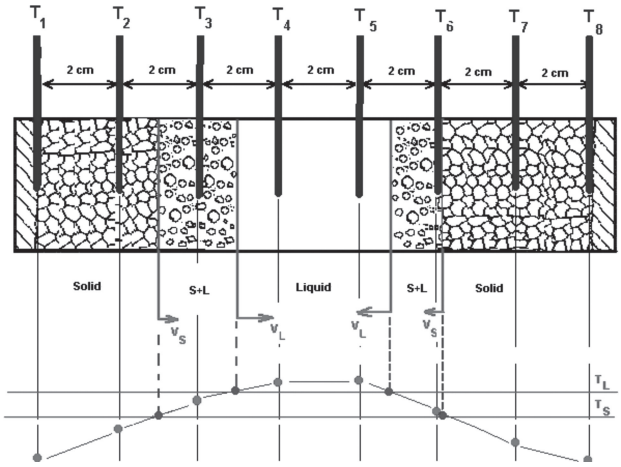

FIG. 1—*Experimental setup (schematic). Eight temperature measurements were used to track [L/(S + L)] and [(S + L)/S] interphases in Zn-Al alloys. The thermocouples are approximately 20 mm apart and the imposed heat flux is toward the ends.*

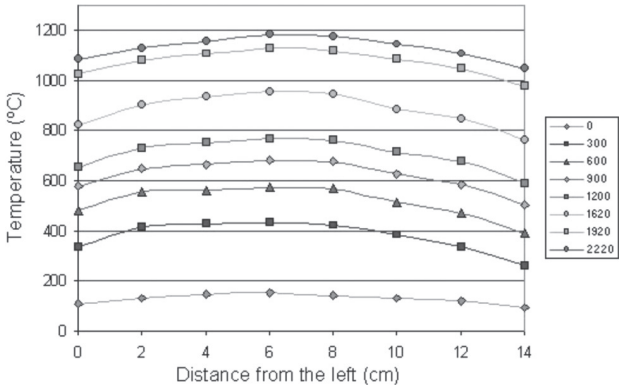

FIG. 2—*Axial temperatures in the horizontal furnace without sample as a function of distance and time measured at eight selected points located in the axis.*

plane, mechanically ground, polished with alumina, and etched with standard reagents to reveal the macrostructures and the microstructures.

Figure 2 shows the thermal gradients as they were measured inside the furnace without the sample. Eight temperature (T) versus time (t) curves were obtained for each running (Fig. 3). Both the onset and the end of solidification in each finite volume were estimated from the change in the slope of the temperature versus time curves, taking the derivatives of each curve. Since the sample is imaginarily divided in eight finite volumes, each thermocouple characterizes the temperature of the whole volume (∼20 mm wide). However, since temperature measurements can be considered representative of a smaller volume, a set of functions were built to interpolate temperatures in-between the thermocouples. Polynomial functions were built to find intermediate temperatures.

The temperature gradients calculated for a Zn-1 wt. %Al sample are shown in Fig. 4. In order to calculate the temperature gradients, the true final position of the thermocouple was measured after solidification.

It is noteworthy that finding the onset and the end of solidification in each volume is not straightforward, since the latent heat released by the volume(s) which is (are) undergoing solidification change(s) the slope of the temperature versus time curves of the remaining thermocouples;

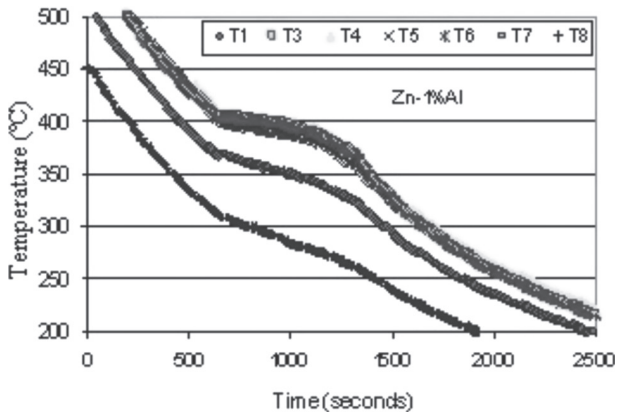

FIG. 3—*Temperature versus time curves as measured in the axis of a Zn-1 wt. %Al sample. The measurements were made at eight selected points located in the longitudinal axis.*

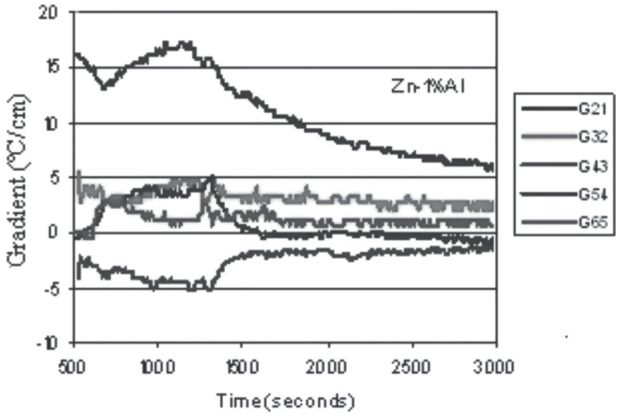

FIG. 4—*Temperature gradients versus time curves as calculated in the axis of a Zn-1 wt. %Al sample. Only five gradients are shown for the sake of clarity.*

thus masking the determination of the onset and the end of solidification in the other still liquid volumes which are heated. Thus, a heated liquid may be mistakenly assumed as the beginning of a mushy zone. Moreover, when solidification concludes in a given volume, the latent heat released by the mushy zone heats up the solid that has already been formed, and thus the end of solidification may appear to be delayed from the "true" ending point. To avoid excessive errors in the determination of the solidification times, we carefully compared each set of temperature measurements with each of the next temperature measurements, back and forth. The first and last thermocouples did not show such displacements in time at the onset of solidification since both ends are the first portions that solidify. In addition, the fourth and fifth thermocouples did not show such displacements in time at the end of solidification since solidification concludes near the middle of the sample and there is no more latent heat released by other zones. The heating of the last portion which ends solidification usually leads to an increase of a few degrees in the temperatures of the remaining thermocouples near the ends for a few seconds after the whole solidification process finishes. We also assumed that the liquidus temperature is not an equilibrium temperature of the alloy, but the onset of the freezing point of the alloy at a non-equilibrium temperature during the cooling of the alloy. Furthermore, solidus or eutectic temperatures are also considered non-equilibrium temperatures because they are the end of the freezing point during the cooling of the alloy. Departures from the equilibrium temperature arise because the temperature measurements were carried out under a dynamic regime of cooling rate, and those departures from equilibrium are less when the cooling rate is lower (i.e., near the center of the sample). The changes in the slope observed just before the onset of solidification are due to the latent heat released far away of the considered volume. This heat also changes the cooling rate in the volume before the volume undergoes the change phase, in such a manner that the cooling rate before the onset of solidification inside the sample is not (and generally should not be) the same as the cooling rate before the onset of solidification at the ends of the sample. The cooling rate before the onset of solidification inside a sample is generally lower than that near the chilled ends or mold walls. This fact should be addressed when modeling solidification structures. Figure 5 shows an example of a change in the slope of a thermocouple measurement at the onset of solidification due to the heating of the neighbouring volume.

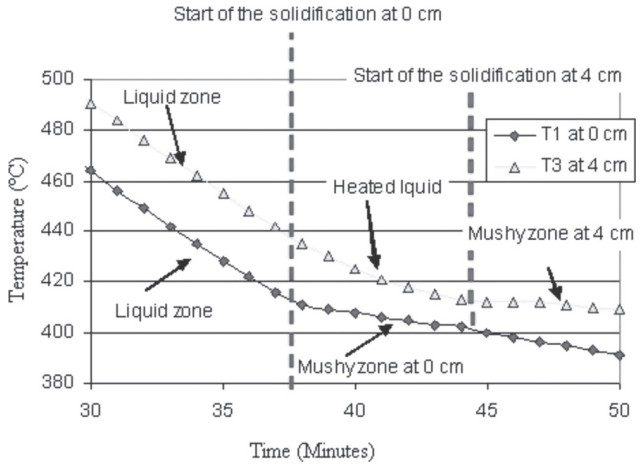

FIG. 5—*Change in the slope of a thermocouple measurement due to latent heat released by a neighbouring volume undergoing solidification. Zn-1 wt. %Al sample. Vertical solidification.*

Figure 6 shows a typical temperature versus time curve with all the features and points which can be used to detect position and time of all the interphases at a given location. Figure 7 shows the derivative of such a curve, or cooling rate, and its characteristic points.

Another fact that has been addressed in directional solidification is that another interphase, such as the [(L + S)/(E + L)] interphase plus the [(E + L)/S] interphase, may be considered when dealing with alloys showing eutectics. The [(L + S)/(E + L)] interphase may be detected when the (solid + liquid) phase reaches the eutectic temperature at the beginning of the isotherm. Also, the [(E + L)/S] interphase runs into the sample at the eutectic temperature measured when the eutectic temperature changes its slope. Figure 8 shows the total local and partial solidification times taking into account the beginning of the eutectic temperature. Thus, the total local solidification times may be split as the sum of the time at which the first solid formed solidifies plus the time for eutectic growth.

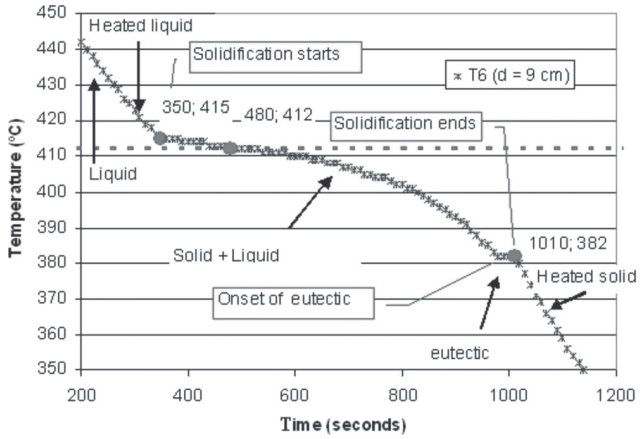

FIG. 6—*Characteristic points and zones in a temperature versus time curve. Zn-1 wt. %Al alloy sample during horizontal solidification, thermocouple T6 (d = 90 mm). It can be observed that some solute segregation exists in the volume because the eutectic plateau clearly appears in the figure.*

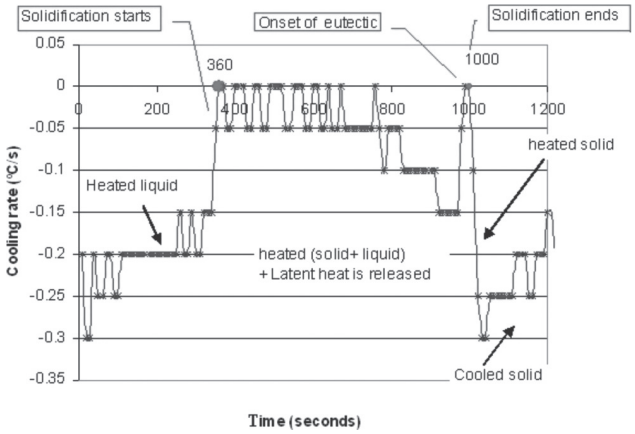

FIG. 7—*Characteristic points and zones in a dT/dt versus time curve. The derivative was taken as centered differences and averaged. Zn-1 wt. %Al sample, horizontal solidification, thermocouple T6 (d = 90 mm). dT/dt = 0 is delayed ±10 s from the onset or from the end since the derivative was taken as centered differences with Δt = 20 s.*

Results and Discussion

Once we made all the previous determinations and calculations, we determined the following functions: (a) a function of time versus distance for the [L/(S + L)] interphase, (b) a function of time versus distance for the [(S + L)/(E + L)] interphases, and (c) a function of time versus distance for the [(E + L)/S] and [(S + L)/S] interphases. In a first approach, we did not consider the splitting of the [(S + L)/S] interphase due to the eutectic growth. Polynomial functions were used to fit near all the points with correlation coefficients greater than 0.9999, and obtain an equation of the time versus distance for each interphase. It is noteworthy that in our case the local solidification time versus solidified distance function cannot be expressed as a quadratic expression, and so the solidified distance is not a single function of the square root of time [9–12].

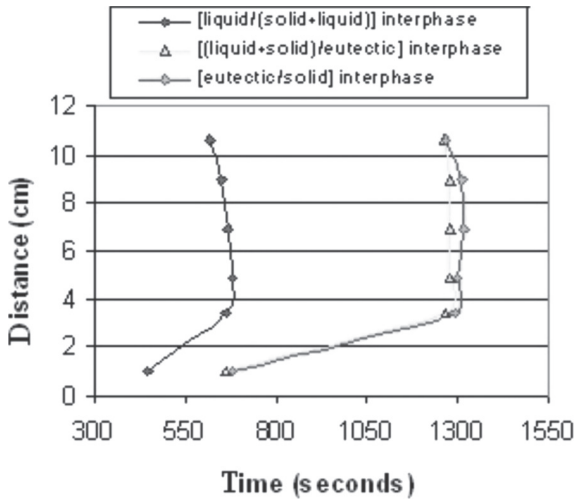

FIG. 8—*Local solidification time curves as measured on the axis of a Zn-1 wt. %Al alloy sample. [L/(S + L)], [(S + L)/(E + L)], and [(E + L)/S] interphases are shown. Only six measurements inside the sample are shown. The heat extraction was from the ends of the sample and not at the same rate.*

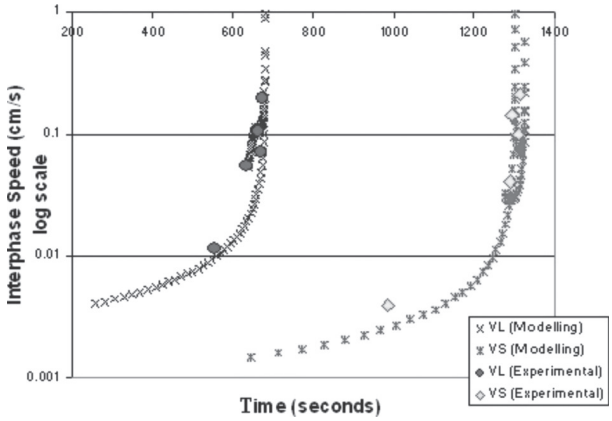

FIG. 9—*Interphase speeds versus time curves for a Zn-1 wt. %Al alloy sample. Horizontal solidification.*

Figure 9 shows the calculated values of the average speed of the [L/(S + L)] and [(S + L)/S] interphases (namely V_L and V_S, respectively), taken as differences between experimental distances ($\cong$ 20 mm) and the time at which the interphases reach the adjacent thermocouples. The speed was also evaluated by other functions such as polynomial functions of fourth and fifth degree (Fig. 9).

It can be seen in this figure that the speed of the interphases increases as solidification progresses. Figure 10 shows both the experimental and simulated average acceleration for the [L/(S + L)] and [(S + L)/S] interphases. Figure 11 shows the average speed as a function of distance for the [L/(S + L)] interphases. The left curve is the experimental average speed for the left to right interphase and the right one is the average speed for the right to left interphase. It is important to point out that both [L/(S + L)] interphases meet between 50 and 51 mm from the left end. Figure 12 shows the averaged speed of the [(S + L)/S] or [(E + L)/S] interphases taken as absolute values for both interphases (left and right).

Note that, when meeting, the [L/(S + L)] interphases reach higher speeds than the [(L + S)/S] interphases. Figure 10 shows an acceleration of the [(S + L)/S] interphases before they collide. However, the average speed of the [(S + L)/S] interphases in the center of the sample shows lower

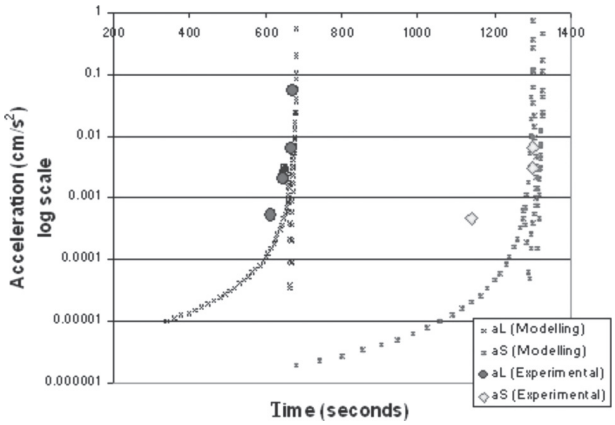

FIG. 10—*Interphase accelerations of a Zn-1 wt. %Al alloy sample. Horizontal solidification.*

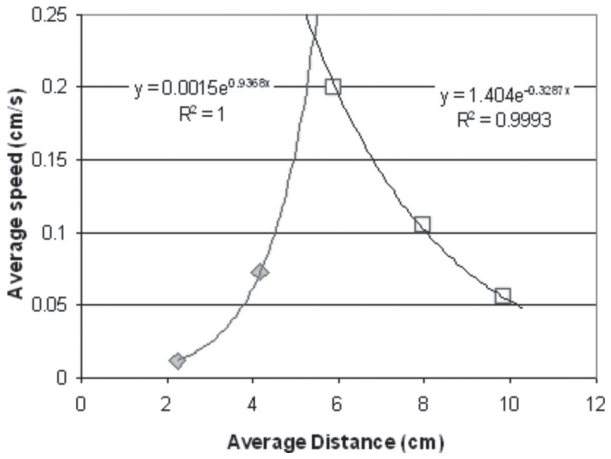

FIG. 11—*Interphase speeds versus distance curves for the [L/(S + L)] interphases of a Zn-1 wt. %Al alloy sample.*

absolute values than at 40 or 80 mm, respectively. The lower speed at the center of the sample is not an effect of a deceleration of the interphase but the speed of another newly born [(S + L)/S] interphase.

In order to find how many interphases exist in the sample, we constructed a plot of the inverse of interphase speed versus distance (Fig. 13).

Figure 13 shows the plot of the functions of V^{-1} versus distance for all the interphases analyzed. Note that the [L/(S + L)] function has a single root, whereas [(S + L)/(E + L)] and [(E + L)/S] have three roots. In order to calculate instantaneous speeds, we built up a set of polynomial functions and interpolated them from the experimental values. Figure 14(*a*) shows only the plot of V^{-1} versus distance for the [L/(S + L)] interphases, whereas Fig. 14(*b*) shows the plot of V^{-1} versus time for the [(S + L)/S] interphases. It can be seen in Fig. 14 that positive values of V^{-1} are taken when a [L/(S + L)] interphase moves from left to right, and that negative values of V^{-1} represent a

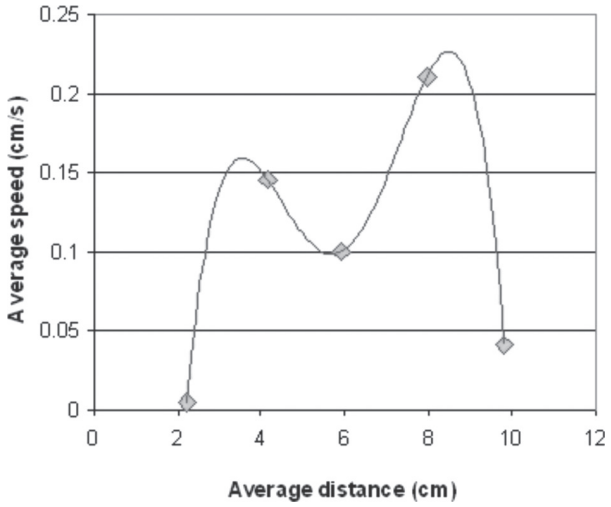

FIG. 12—*Interphase speeds versus distance curves for the [(E + L)/S] interphases of a Zn-1 wt. %Al alloy sample. Horizontal solidification. Experimental (absolute values).*

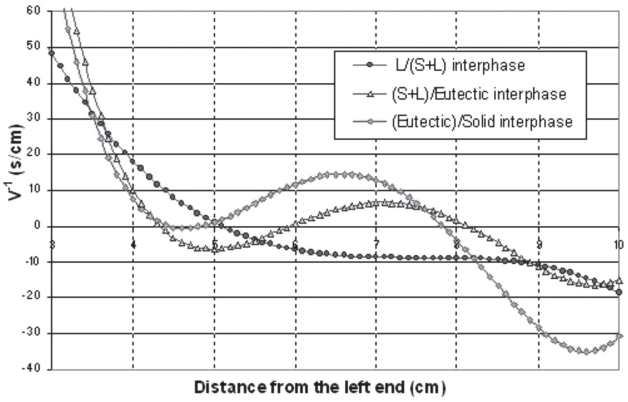

FIG. 13—*Plot of V^{-1} versus distance for the six interphases analyzed in this work. Positive values of 1/V indicate interphases moving from the left to the right. Negative values of 1/V indicate interphases moving from the right to the left.*

[L/(S + L)] interphase moving from right to left. Figure 14(*b*) shows that there is a single time where two [L/(S + L)] interphases collide, leaving a whole mushy zone inside the sample.

Figure 13 also shows the plot of V^{-1} versus distance for the [(S + L)/S] interphases. The intersection with the abscise axis gives the approximate positions for the collision.

Figure 15(*a*) shows the plot of V^{-1} versus time for the [(S + L)/S] interphases. As it can be seen in Fig. 15(*a*), there is an instant at which the left [(S + L)/S] interphase having positive speed values reaches negative values. This is neither an effect of deceleration of the interphase nor a change of direction, but the creation of a new [(S + L)/S] interphase inside the mushy zone. Thus, crystallization isotherms will duplicate each time after a new [(S + L)/S] interphase is created. Looking at Fig. 15(*a*) in detail, it can be seen that there are three instants at which $1/V_S \rightarrow 0$, i.e., $V_S \rightarrow \infty$. However, this is only an effect of assuming a single function for all the [(S + L)/S] interphases. The latter can be observed in Fig. 15(*b*), which is a close-up of Fig. 15(*a*) near the instant of creation of new interphases.

Figure 15(*b*) shows that two new [(S + L)/S] interphases emerged at 1299.96 s (arbitrary zero) at a distance of 48 mm from the left and met the [(solid + liquid)/solid] interphase running from the left. This collision occurs at 1300.1 s at a distance of 45 mm. The opposite interphase born at

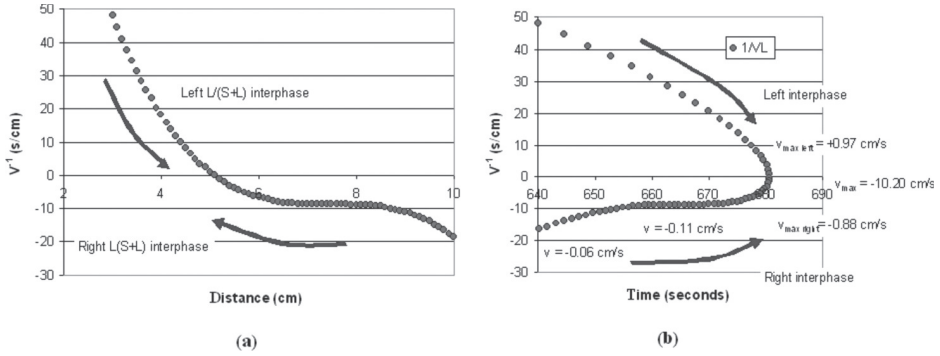

FIG. 14—*(a) Plot of V^{-1} versus distance for the two [L/(S + L)] interphases analyzed in this work. (b) Plot of V^{-1} versus time for the two [L/(S + L)] interphases. Positive values of $1/V_L$ indicate interphases moving from the left to the right. Negative values of $1/V_L$ indicate interphases moving from the right to the left.*

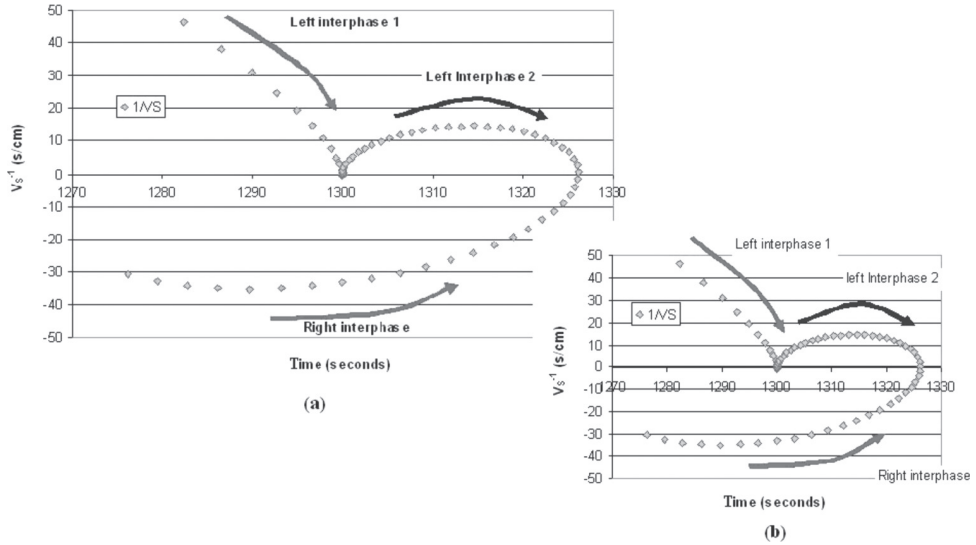

FIG. 15—*(a) Plot of V^1 versus time for the [(E + L)/S] interphases. Positive values of $1/V_S$ indicate interphases moving from the left to the right. Negative values of $1/V_S$ indicate interphases moving from the right to the left. (b) Enlargement of (a) around the time of creation of two new [(E + L)/S] interphases, one of which collides with the interphase running from the left.*

1299.96 s departs from a distance of 48 mm, having positive speed and moves from left to right. It eventually substitutes the previous left-running interphase. The high velocities at the beginning of the creation of the interphases seem to be unrealistic and only a mathematical effect due to the fact that a single function was taken to simulate all the interphases. However, time and distances seem to be computed more accurately. Once times and approximate positions of the creations and collisions of such interphases were determined, in order to estimate velocities more accurately we split the overall function in a set of several functions, taking a single function for each interphase of the same kind. Taking a single function for each interphase gives low velocity values at the time of creation. Besides, time and distances for the creation and collision of interphases give values similar to the previous one. Figure 16 shows the calculated speeds of the [(S + L)/S] interphases, as determined by a set of single functions. The [(S + L)/S] interphases created inside the sample begin

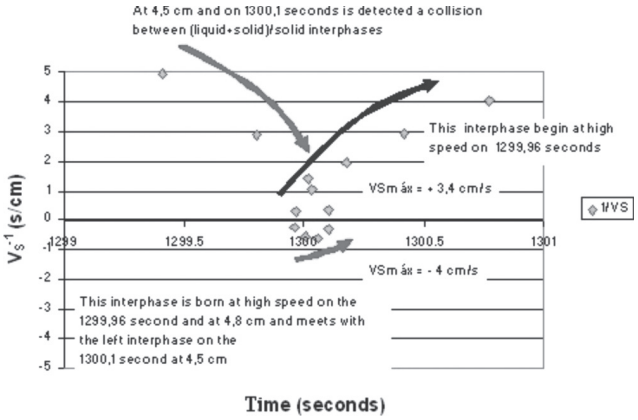

FIG. 16—*Calculated speeds as a function of distance for [(S + L)/S] or [(E + L)/S] interphases.*

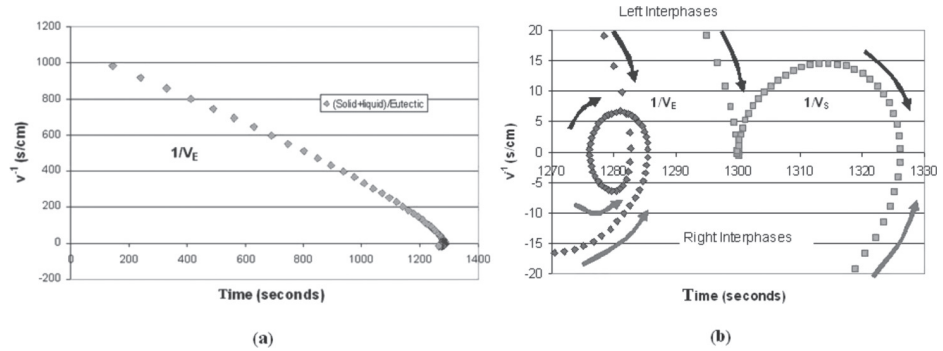

FIG. 17—*(a) Plot of V_E^{-1} versus time. (b) Enlargement of (a) showing the instant of creation of two new [(S + L)/(E + L)] interphases one of which collides with the interphase running from the left.*

at ±0.4 mm/s and collide with the initial solid interphases at a maximum speed of 3.66 mm/s with the interphase running from the left, and at a maximum speed of 6.8 mm/s with the initial [(S + L)/S] interphase running from the right. Note that, by the time of collision, both interphases undergoing the interaction have similar speed values (3.65 and −3.66 mm/s) as well as 23.1 and −16.5 mm/s).

We also noticed that the solidified fraction of the sample shows an abrupt increase as a consequence of this solid which appears suddenly inside the sample. This is due to the fact that tracking a single [(S + L)/S] interphase does not take into account newly born interphases inside the mushy zone.

Moreover, by analyzing in detail the [(S + L)/(E + L)] interphases, we found a similar behaviour [Fig. 17(*a*) and 17(*b*)]. The [(S + L)/(E + L)] interphase is not created just at the onset of the solidification, because the Zn-Al alloy used in these experiments has only 1 wt. % of Al, and the first solid formed reaches the solidus temperature or the eutectic plateau at a very short time at the beginning. The segregation of Al increases the solute concentration in the center of the sample and the isoline shows a longer plateau from thermocouples *T*3 to *T*6. Figure 17(*b*) shows the position and the time where the new [(S + L)/(E + L)] interphases were born and the position and the time for the collision.

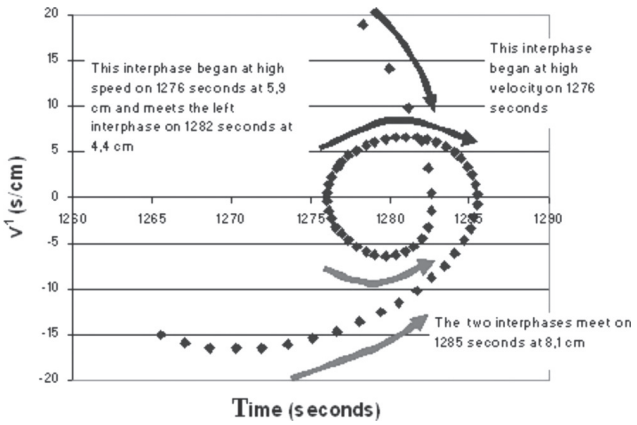

FIG. 18—*Plot of V^{-1} versus time for the [(S + L)/(E + L)] and [(E + L)/S] interphases.*

TABLE 1—Calculated values of maximum speeds and maximum accelerations just before collision for all the interphases running in a Zn-1%Al horizontal sample.

Interphase	Movement	Time before collision (s)	Distance from the left (cm)	Maximum speed (absolute values) (cm/s)	Maximum acceleration (absolute values) (cm/s^2)
[L/(S + L)]	Left to Right	682.2	4.50	0.270	0.377
[L/(S + L)]	Right to Left	672.3	6.00	3.465	28.417
[(S + L)/(E + L)]	Left to Center	1282.6	4.30	1.608	6.788
[(S + L)/(E + L)]	Center to Left	1282.5	4.40	0.676	1.548
[(S + L)/(E + L)]	Center to Right	1285.5	8.10	2.567	20.097
[(S + L)/(E + L)]	Right to Center	1285.4	8.20	1.248	5.328
[(E + L)/S]	Left to Center	1309.8	4.20	0.365	0.918
[(E + L)/S]	Center to Left	1309.6	4.30	0.366	0.309
[(E + L)/S]	Center to Right	1321.8	7.50	2.310	37.667
[(E + L)/S]	Right to Center	1321.8	7.60	1.650	6.335

Figure 16 shows that two new [(S + L)/(E + L)] interphases were born at 1276.0 s (arbitrary zero) at 59 mm from the left end and that they meet a previous [(S + L)/(E + L)] interphase running from the left at 1282.0 s at 43–44 mm. The parent interphase moving to the right was born at 1276.0 s at 59 mm and meets the right interphase at 1285.0 s at 81−82 mm calculated from the left.

A graph of V^{-1} versus time for the [(S + L)/(E + L)] and [(E + L)/S] interphases is shown in Fig. 18. It can be observed that the [(S + L)/(E + L)] interphases were born first and collided before the [(E + L)/S] interphases were created inside the sample.

It is noteworthy that while the [L/(S + L)] interphases start at the liquidus temperature and is assumed that such interphase is at a non-equilibrium liquidus temperature, this liquidus temperature may change due to local solute rejection. Thus, some errors in the determination of position may be due to local change in the liquidus temperature of the alloy locally. In this work, we did not take into account the change in the liquidus temperature due to segregation. However this fact does not invalidate the previous analysis since the position of the interphases are taken from the cooling rate curves that derive from the temperature versus time curves and not from the interphase temperatures. Further research is being carried out to find suitable functions for the characteristic temperatures, as a function of distance, time and local cooling rate before phase transition.

Table 1 summarizes the calculated maximum speeds and maximum accelerations before collision for all the interphases present in a Zn-1 wt. %Al system with chilled ends undergoing one-directional horizontal solidification.

Summary and Conclusions

Four kinds of behaviors were experimentally found for zinc-aluminum alloys in one-directional solidification: (a) two interphases; (b) three interphases; (c) four interphases and; (d) six interphases of solidification. In the present work, we analyzed one-directional solidification with two heat flux extractions, which provides a system with six basic interphases, three of which move from left to right, and three of which move from right to left. Besides, new interphases that move toward the chilled ends are created inside the alloy. Thermal and kinetic conditions, interphase speeds and accelerations were measured and calculated numerically by modeling. Although a system with eight interphases may occur, we did not find it in our experiments. Furthermore, it can be noticed that

local solidification time follows a set of different functions depending on the number of interphases present in the system.

If the alloy shows a [(S + L)/(E + L)] interphase, this interphase appears in-between the zone delimited by the [L/(S + L)] and [(S + L)/S] interphases in a plot of distance versus time. In zinc-aluminum alloys with a low content of Al this can be found for concentrations of aluminum ranging between 1 % wt. and 5 % wt.

From the present work it may be concluded that:

1. During the directional solidification of a binary alloy which does not show a eutectic temperature, it is possible to identify at least two kinds of interphases: [L/(S + L)] and [(S + L)/S].
2. During the directional solidification of a binary alloy showing a eutectic temperature, it is possible to identify at least three kinds of interphases: [L/(S + L)], [(S + L)/(E + L)] and [(E + L)/S].
3. If the horizontal solidification of the binary alloy showing a eutectic temperature is one-directional and with double heat extraction (i.e., chilled from both ends), it is possible to identify at least six interphases: two [L/(S + L)] interphases, two [(S + L)/(E + L)] interphases, and two [(E + L)/S] interphases, three of which run from left to right and three of which run from right to left.
4. When a binary alloy undergoing solidification reaches a eutectic temperature, the isotherm is not a single line in space but a volume where temperature is constant. Thus, isotherms are not cut among itself, but many isotherms may have the same value. Many "interfaces" can exist in the (solid + liquid) phase inside this volume, and can move in an isothermal field.
5. Local changes in the thermal field inside a binary alloy sample undergoing solidification may lead to the growth of new [(S + L)/S] interphases which rapidly grow toward the ends and collide with the advancing fronts coming from the ends. The speed of those newly born interphases is not constant and exists at a time-dependent acceleration field. Interphases may be born with null or small speed; once they are created they increase their speeds before they collide.
6. The distances and the times of creation of the new interphases, and the prevailing local thermal and kinetic conditions can be determined by local measurements of temperature versus time. However, in order to be able to detect them, the acquisition interval should be very short (less than 1 s per channel), since some interphases may have very short life time ($\sim$0.1 s).
7. By the time of collision, interphases seem to have very high speeds when only one function is used to simulate all the interphases of the same kind. Mathematically, the speeds tend to infinity, but such high averaged speeds were not found experimentally. The individual functions for the speed of each interphase seem to follow an exponential law with distance and the high speed when meeting become null almost instantaneously after collision. For [L/(S + L)] interphases, the calculated values of such speed just before collision were -34.65 and $+2.7$ mm/s. However, the determinations of the averaged speeds in our experiments showed that interphase speeds higher than 2.5 mm/s (average value) are difficult to occur.
8. By the time new [(S + L)/(E + L)] interphases are created inside the mushy zone, liquid phase still remains, and the whole solidification process occurs later when [(E + L)/S] interphases meet. Eutectic growth starts at different times at different locations, and more than two [(S + L)/(E + L)] averaged interphases may exist simultaneously at different locations and moving in opposite directions.
9. The speeds of the [(S + L)/(E + L)] interphases are not constant in time or in position. By the time the newly born [(S + L)/(E + L)] interphase moving from the center to the right collides with the prior [(S + L)/(E + L)] interphase moving from right to left, the maximum calculated speeds were $+26$ and -12 mm/s, respectively. By the time the newly born [(S + L)/(E + L)] interphase moving from the center to the left collides with the prior [(S + L)/(E + L)] interphase

moving from left to right, the maximum calculated speeds just before collision were −7 and +16 mm/s, respectively.

10. By the time of collision, or end of the whole solidification process, the calculated instantaneous speeds of the two interphases [(E + L)/S] undergoing interaction were +23 and −16.5 mm/s, respectively. However, the averaged speed as determined by direct measurements of distances and time showed average values in the order of 2.1 mm/s.
11. Accelerations of interphases do not have a constant value and the acceleration increases as the movement of the interphase progresses, reaching the highest values before collision.
12. The geometric point (or surface) where the [L/(S + L)] interphases meet does not necessarily coincide with the geometric point (or surface) where the [(S + L)/(E + L)] interphases meet or with the geometric point where the [(S + L)/S] interphases meet inside a sample.
13. We found that the [(E + L)/S] interphases can be created inside a sample and run toward the chilled ends, leaving an internal solid zone. In directional solidification we found this situation only after a eutectic temperature or isoline is reached inside the sample.

Acknowledgments

This project was partially financed by PICT-O No. 36866. The writers thank Consejo Nacional de Investigaciones Científicas y Técnicas, CONICET (Argentina), for the financial support. The writers thank Mr. Ferrari for setting up the cooling system and piecing the metals used in the experiments. Help from glass blower of the Facultad de Ciencias Exactas, Químicas y Naturales-Universidad Nacional de Misiones, FCEQyN-UNaM, is gratefully acknowledged.

References

[1] Trivedi, R. and Somboonsuk, K., "Constrained Dendritic Growth and Spacing," *Mater. Sci. Eng.*, Vol. 65, 1984, pp. 65–74.

[2] Somboonsuk, K., Mason, J. T., and Trivedi, R., "Interdendritic Spacings; Part 1: Experimental Studies," *Metall. Trans A* Vol. 15, 1984, pp. 967–975.

[3] Reinhart, G., Mangelick-Noël, N., Nguyen-Thi, H., Schenk, T., Gastaldi, J., Billia, B., Pino, P., Härtwig, J., and Baruchel, J., "Investigation of Columnar-Equiaxed Transition and Equiaxed Growth of Aluminium Based Alloys by X-Ray Radiography," *Mater. Sci. Eng. A*, Vol. 413–414, 2005, pp. 384–388.

[4] Mangelinck-Noël, N., Nguyen-Thi, N., Reinhart, G., Schenk, T., Cristiglio, V., Dupouy, M. D., Gastaldi, J., Billia, B., Härtwig, J., and Baruchel, J., "In Situ Analysis of Equiaxed Growth of Aluminium–Nickel Alloys by X-Ray Radiography at ESRF," *J. Phys. D: Appl. Phys.*, Vol. 38A, 2005, pp. 28–32.

[5] Mathiesen, R. H. and Arnberg, L., *Modeling of Castings, Welding and Advanced Solidification Process, In-situ Experimental Observations of Dendritic Growth in Al-Cu Alloys*, The Minerals, Metals and Materials Society (TMS), Destin, FL, 2003, pp. 677–684.

[6] Schenk, T., Nguyen-Thi, H., Gastaldi, J., Reinhart, G., Cristiglio, V., Mangelinck-Noël, N., Klein, H., Härtwig, J., Billia, B., and Baruchel, J., "Application of Synchrotron X-Ray Imaging to the Study of Directional Solidification of Aluminium-Based Alloys," *J. Cryst. Growth*, Vol. 275, 2005, pp. 201–208.

[7] Grange, G., Jourdan, C. Gastaldi, J. and Billia, B., "Strain Visualization of the Onset of Morphological Instability and Defect Formation in Cellular Solidification of a Dilute Al-Cu Alloy," *Acta Mater.*, Vol. 45, 1997, pp. 2329–2338.

[8] Borelli, R. S., Bonczock, A., Candia, A. E., Ares, A. E., and Gueijman, S. F., "Análisis del Comportamiento de las Interfases con dos Sentidos de Movimiento en la Solidificación Unidireccional de Aleaciones Zinc-Aluminio," *Proceedings of the Segundo Encuentro de Jóvenes Investigadores en Ciencia y Tecnología de Materiales*, Posadas, Misiones, Argentina, 2008.

[9] Pires, O. S., Prates, M., and Biloni, H., "Unidirectional Solidification of Metals with Zero Superheat. Case of Cooled Molds," *Z. Metallkd. Bd. H.*, Vol. 65(2), 1974, p. 143.

[10] Lipton, J., Garcia, A., and Heinemann, W., "An Analytical Solution of Directional Solidification with Mushy Zone," *Arch. Eisenhüttenwes.*, Vol. 53(12), 1982, pp. 469–473.

[11] Clyne, T. W. and Garcia, A., "Assessment of a New Model for Heat Flow During Unidirectional Solidification of Metals," *Int. J. Heat Mass Transfer*, Vol. 23, 1980, pp. 773–782.

[12] Garcia, A., Clyne, T. W., and Prates, M., "Mathematical Model for the Unidirectional Solidification of Metals II. Massive Molds," *Metall. Trans. B*, Vol. 10, 1979, pp. 85–92.